

**Initial events in bovine coronavirus infection:
analysis through immunogold probes and lysosomotropic inhibitors**

H. R. Payne¹, J. Storz¹, and W. G. Henk²

Departments of ¹Veterinary Microbiology and Parasitology and of ²Veterinary Anatomy and Fine Structure, Louisiana State University, Baton Rouge, Louisiana, U.S.A.

Accepted May 14, 1990

Summary. The early events in the infection of human rectal tumor cells by bovine coronavirus were investigated by colloidal gold-mediated immunoelectron microscopy and by analysis of the effect of lysosomotropic weak bases on virus yield. Electron microscopic studies revealed sites of fusion between the virus envelope and the plasmalemma but fusion events along intracellular membranes were not observed despite extensive searches. Virion-antibody-colloidal gold complexes were, in fact, endocytosed by synchronously infected cells. These complexes were apparently non-infectious, and they accumulated in vacuoles that resembled secondary lysosomes. Exposure of cells to ammonium chloride or to methylamine during the first hour of infection had little inhibitory effect on the production of infectious virus. Chloroquine treatments were inhibitory but this effect depended on relatively late events in the infectious process. The chloroquine inhibitory step blocked infection of virus adsorbed to cells that were exposed to buffers in the pH range of 4.4 to 8.4. These findings indicate that BCV penetrates its host cell by direct fusion with the plasmalemma and does not require an acidic intracellular compartment for infectious entry.

Introduction

Bovine coronavirus (BCV) is a member of the family *Coronaviridae* of enveloped RNA viruses [31]. The BCV isolates studied in some detail agglutinate erythrocytes of rodents and thus belong to the hemagglutinating coronaviruses. Uniquely, the envelope of these coronaviruses has three glycoproteins. The peplomers consist of the E1 membrane glycoprotein with a molecular mass of 24–26 kDa, the E2 glycoprotein with a molecular mass of 100–110 kDa which has cell fusion functions after cleavage from 185 kDa precursor [34] and the E3 hemagglutinin with a molecular mass of 65 kDa or its dimer of 126 kDa. Acetylerase activity is associated with this hemagglutinin [38]. BCV replicates

in absorptive epithelial cells of the intestinal tract in neonatal calves and induces serious enteric disease [11]. Although many features of coronavirus replication in cultured cells were described [10, 30, 32], the early events of BCV infection remain poorly characterized.

At least, two distinct pathways evidently operate for the entry of enveloped viruses into animal cells [15]. Some viruses penetrate the cell by direct fusion of the viral envelope with the plasma membrane. Paramyxoviruses, for example, fuse directly with the cellular plasma membrane under physiological conditions [28]. Other viruses fuse with plasma membranes only at a nonphysiological, low pH level [7, 8, 20, 40]. The second pathway for enveloped virus entry involves cellular uptake by endocytosis [8, 17–20]. The endocytosed virions travel to membrane bound intracellular compartments where acidic conditions are maintained [25, 37]. The low pH of this cellular compartment apparently facilitates fusion between the viral envelope and the vesicle membrane and results in release of the nucleocapsid into the cytoplasm. Infection of cultured cells by a variety of enveloped viruses can be blocked with lysosomotropic weak bases [8, 9, 12, 14, 18, 20, 22, 24]. These bases accumulate in cells and alter the pH of acidic cellular compartments [21, 25]. This change apparently prevents low pH-dependent viral envelope fusion with the vesicle membrane and thus blocks infection [9].

Studies of inhibition by lysosomotropic agents indicate an endocytic mechanism for the entry of mouse coronavirus [14, 16, 22, 36], but the validity of this approach has recently been questioned [2]. Low pH conditions may not be required for BCV entry because cells infected with this virus fuse under slightly basic pH conditions [27]. In order to establish the route of entry for BCV, we examined the early events of the infection process by using lysosomotropic weak bases and colloidal gold mediated immunoelectron microscopy.

Materials and methods

Cells and virus

Monolayers of the human rectal tumor cell line HRT-18 [35] were grown in the Dulbecco modification of Eagle medium (DMEM) supplemented with 5% fetal calf serum. The Mebus strain L9 of bovine coronavirus [29] was propagated in HRT-18 cells. Virus stocks were prepared in cells infected at a multiplicity of approximately 0.01 PFU per cell, incubated for 4 to 5 days at 37 °C in serum-free DMEM and harvested by freeze-thawing. Viral titers obtained in these preparations ranged from 10⁶ to 10⁷ PFU per ml.

Plaque assays

The infectivity titer was assayed in HRT-18 monolayers grown in 6-well plates. The monolayers were adsorbed with virus for 1 h at 37 °C, overlaid with serum-free DMEM containing 0.6% agarose and 4 µg of trypsin (Difco Laboratories, Detroit, Mich.) per ml. After 3 days of incubation at 37 °C, plaques were counted without staining.

Virus purification and concentration

Infected cultures were harvested at 4 d post infection when more than 50% of the cells evidenced cytopathic changes. The infected material was subjected to two freeze-thaw cycles and disrupted by sonication (Sonifier 200; Branson Sonic Power Co., Danbury, Conn.) for 30 sec on ice to release the virus. The virus suspension was clarified by centrifugation at $10,000 \times g$ for 40 min, sedimented at $90,000 \times g$ for 2 h through a 20% sucrose cushion, and resuspended in DMEM (pH 7.4) buffered with 12 mM N-2-hydroxyethylpiperazine-N'-2-ethanesulfonic acid (HEPES) and 25 mM NaHCO_3 (uptake medium). The recovery of infectious virus ranged from 50 to 75%.

Immunoreagents

We used a polyclonal rabbit antibody against BCV particles purified from infected bovine fetal kidney cells. The IgG fraction was obtained by protein-A sepharose column chromatography and was diluted in uptake medium to a level producing less than a 50% reduction of virus infectivity as determined by a plaque neutralization test. Goat anti-rabbit antibody (IgG) complexed to 5-nm colloidal gold particles (SP Supplies, West Chester, Penn.) was used to probe for antibody binding sites in immunocytochemical investigations.

Immunogold labelling of virus entry

Cell monolayers, grown in 2-well chamber slides, were rinsed with uptake medium, chilled to 4 °C, and reacted with purified virus for 60 min at a multiplicity of 50 PFU per cell. The virus-cell complexes were incubated on ice for 45 min with rabbit anti-BCV antibody, washed twice with uptake medium, and incubated for 45 min with the antibody-colloidal gold probe. After washing at 4 °C, the cells were rapidly warmed to 37 °C and incubated for various lengths of time before primary fixation at 4 °C with 2% glutaraldehyde and 2% formaldehyde in 0.1 M sodium cacodylate buffer at pH 7.4.

Processing for electron microscopy

The aldehyde-fixed monolayers were post-fixed for 1 h at 25 °C in a solution of 1% osmium tetroxide in the presence of 1% potassium ferrocyanide in 0.1 M cacodylate buffer (pH 7.4), dehydrated in a series of alcohols, and embedded in situ in a mixture of Epon and Araldite epoxy resins [23]. Thin sections were stained with uranyl magnesium acetate and lead citrate and viewed with a Zeiss EM-10 electron microscope at 80 kV.

Effects of lysosomotropic bases on BCV infection

Monolayers of HRT-18 cells were grown in 24-well plates for experiments involving treatments with lysosomotropic agents. The yields of infectious virus were determined by plaque assays after 20 h of infection at 37 °C.

Infection of HRT-18 cells was synchronized by temperature shift to analyze the relative effects of chloroquine, ammonium chloride, methylamine, and amantadine. Monolayers were washed with medium, chilled to 4 °C, adsorbed for 60 min with BCV at a multiplicity of approximately 3 PFU per cell, and rinsed with cold uptake medium to remove unadsorbed virus. The monolayers were given warm medium with the appropriate lysosomotropic bases and transferred to a 37 °C incubator. In control monolayers, exposure to the base was delayed until 1 h post infection.

The effects of various concentrations of ammonium chloride and chloroquine in virus infection at 37 °C were tested on monolayers that were washed with uptake medium and pretreated for 15 min with the base diluted in uptake medium. The cells were infected with BCV at 37 °C for 60 min at a multiplicity of approximately 3 PFU per cell and then given

fresh uptake medium containing the base. Exposure to the lysosomotropic agent was delayed until 1 h post infection in control monolayers.

The time dependence of inhibition by 120 μ M chloroquine was analyzed by measuring the effects of increasing delays in chloroquine addition. The monolayers were synchronously infected as described above except that chloroquine was first added to the cultures at various times after rewarming.

The pH dependence of chloroquine inhibition was determined with monolayers that were allowed to bind BCV at 4 °C and then were washed with cold DMEM. The cells were warmed to 37 °C for 60 sec by the addition of DMEM buffered with 12 mM HEPES and 12 mM 2-(N-morpholino-)ethanesulfonic acid (MES) at various pH levels and given fresh uptake medium with 120 μ M chloroquine. Chloroquine was added at 1 h post infection for a final concentration of 120 μ M in all monolayers.

Indirect immunofluorescence

Monolayers were fixed for 10 min in 4% formaldehyde, permeabilized for 5 min with acetone at -20 °C, incubated with rabbit anti-BCV antibody, and reacted with goat anti-rabbit antibody conjugated to fluorescein isothiocyanate. The preparations were viewed with a Leitz fluorescent microscope and each field was photographed using both epifluorescence and phase contrast optics. The percentage of fluorescent cells in each preparation was calculated from 5 randomly selected fields of approximately 200 cells each.

Chemicals

Stock solutions were prepared daily of 20 mM chloroquine-HCl, 200 mM amantadine-HCl, 1.0 M ammonium chloride, and 4.0 M methylamine (Sigma Chemical Co., St. Louis, Mo.) in saline. The solutions were adjusted to neutral pH with NaOH, and diluted into uptake medium.

Results

Morphologic analysis of BCV adsorption

Thin section of cells adsorbed with BCV particles and immunolabeled at 4 °C revealed that coated pit formation had ceased leaving all virions at the cell exterior (Fig. 1). The virions were readily identified by the associated colloidal gold particles. The use of highly dilute anti-BCV antibody labeled most virions with only a few gold particles. These particles were separated from the viral envelope by an average distance of about 15 nm. The virus particles usually contained an electron-dense core and were spherical in shape with diameters ranging from 50 to 80 nm. Virions with ellipsoidal profiles also were observed. The viral envelope was separated from the plasma membrane by a distance of less than 15 nm in many cases. Fibrillar connections were evident at the plasma membrane attachment site (Fig. 1, inset) but the peplomer structures of BCV, distinctive in negative stains, could rarely be distinguished. The virus particles were unevenly distributed among the cells. Most cells in individual thin section were free of virus particles or were associated with only one or two virions. Other cells were observed with as many as 25 virions along the apical cell surface in a single thin section. This distribution infers that virus particles were adsorbed by only a subpopulation of HRT-18 cells in the monolayer.

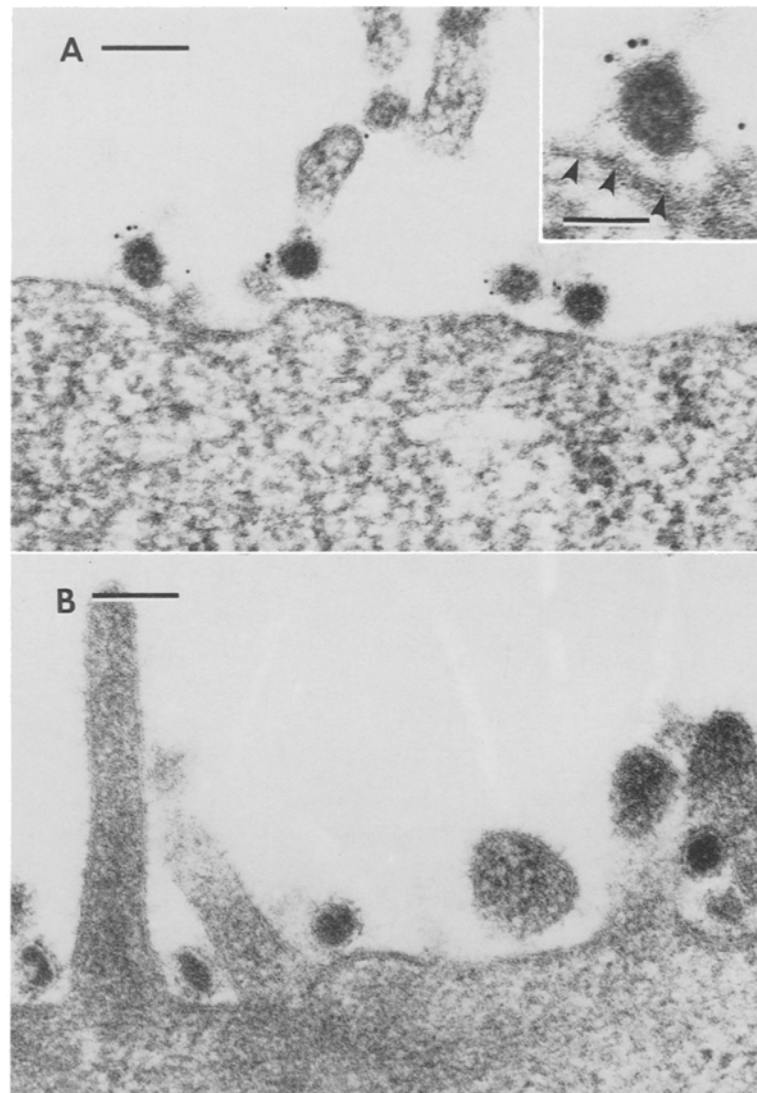


Fig. 1. Immunoelectron microscopic analysis of BCV interaction with the plasma membrane at 4°C. **A** Virus particles are labeled with gold. Envelope projections contact the cell membrane (inset, arrowheads). **B** Gold particles fail to bind with virions in preparations incubated with normal rabbit serum IgG. Bars: 100 nm, inset bar: 50 nm

Endocytosis of BCV at 37°C

Virus particles at intracellular locations were morphologically less readily distinguished, but the associated gold label permitted identification of intracellular BCV particles during uptake. After the BCV-cell complexes were incubated for 2 to 5 min at 37°C, labeled BCV particles were evident in coated vesicles and in small multiform vesicles with smooth membranes (Fig. 2).

Coated vesicles had circular profiles of 100 nm in diameter, whereas the smooth membrane vesicles were typically larger (160 to 300 nm in the greater

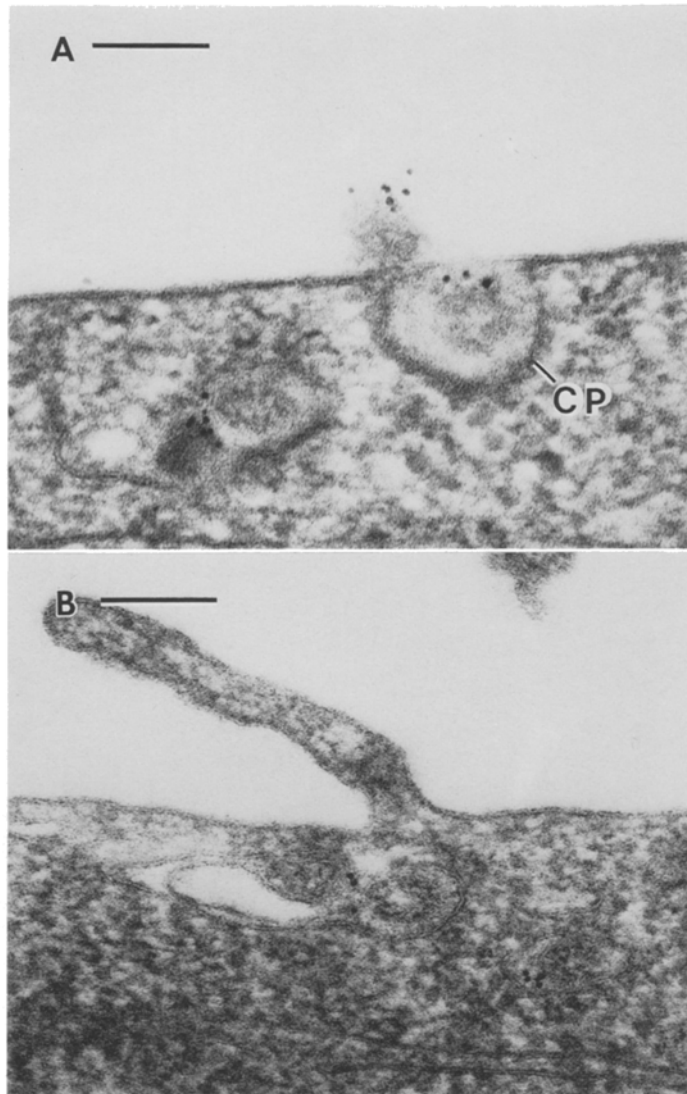


Fig. 2. Early stages of BVC internalization. Monolayers were warmed for 2 min (A) or 5 min (B). Immunogold labeled virus particles are found in a coated pit (CP). Bars: 100 nm

dimension) and had diversely shaped profiles. These membranous compartments contained only one or two virus particles but had very little empty space and few nonviral content. After 10 to 15 min incubation at 37 °C, the intracellular virions accumulated in larger vacuoles, 400 to 800 nm across (Fig. 3). These vacuoles contained as many as 10 labeled virus particles which appeared to be partially degraded. The large vacuoles also contained unlabeled vesicles, fibrillar strands, and amorphous material, features of secondary lysosomes.

Gold particles were closely associated with virus structures and were separated from the nearest limiting cellular membrane by distances exceeding 20 nm.

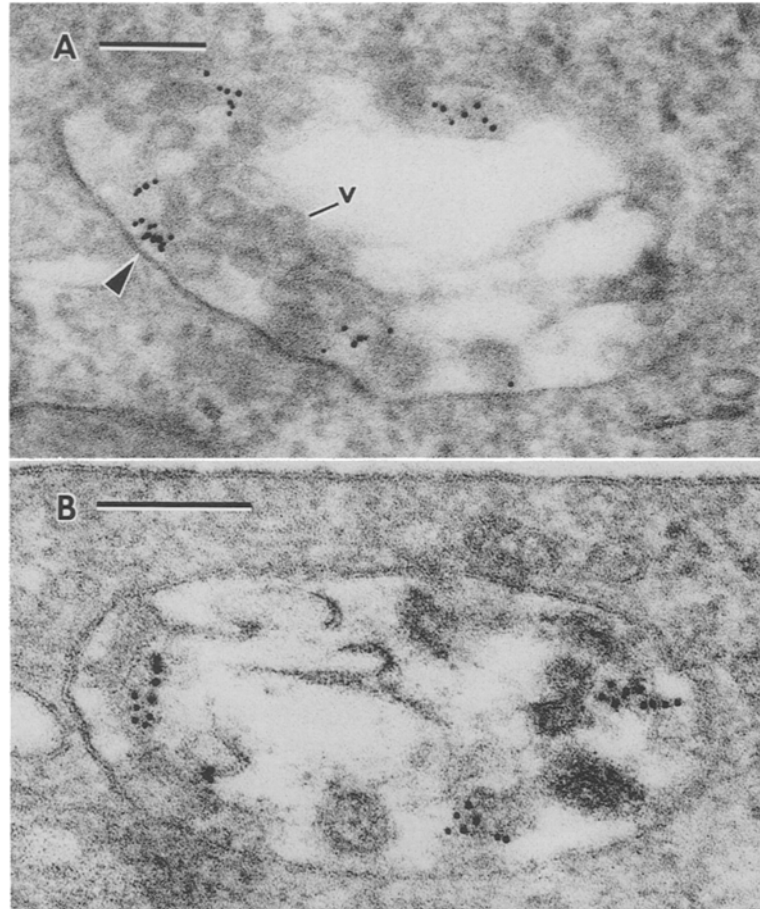


Fig. 3. Accumulation of BCV inside vacuoles. Virus-cell complexes were incubated for 10 min (**A**) or 15 min (**B**) at 37°C. Electron dense particles associated with gold represent partially degraded virions. Vacuole contents also include unlabeled vesicles (*v*) and fibrillar debris. Note possible site of gold association with vacuole membrane (\blacktriangleleft). Bars: 100 nm

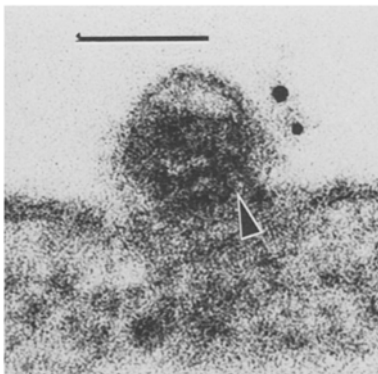


Fig. 4. Interaction of BCV envelope with plasma membrane. Virus cell complexes were rewarmed for 30 sec. \blacktriangleright Site of apparent fusion. Bar: 50 nm

Associations between gold particles and vesicle membranes were rarely seen (Fig. 3). After rewarming, gold particles were observed at plasma membrane sites distant from adsorbed virions. Apparent fusion of the virus envelope with the plasma membrane was recorded (Fig. 4), but fusion of gold-labeled virions with intracellular membranes was never observed. Cells with surface-adsorbed virus that were incubated with normal rabbit IgG instead of anti-BCV antibody were not labeled by the gold probe (Fig. 1B).

Furthermore, few gold particles were observed at plasma membrane sites in the absence of virus particles when virus-cell complexes were immunolabeled and fixed at 4 °C. These controls indicated that the immunoreagents specifically marked BCV antigens and not HRT-18 cell membranes.

Effect of lysosomotropic agents on the yield of infectious virus

To compare the effect of bases, synchronously infected cells were treated with chloroquine, amantadine, ammonium chloride or methylamine (Table 1) at concentrations previously found to be effective in studies of virus entry [8, 12, 20, 24]. Treatment with a given base was continued until virus harvest. Virus yields were reduced to some extent by each of the inhibitors. The degree of the reduction by each inhibitor depended on the duration of the treatment period. We measured virus yields of cultures treated from the time of infection and compared these values to yields in cultures first exposed to the inhibitor at 1 h post infection. The latter value provided a baseline from which we could evaluate the effects of the inhibitor during the first hour of infection.

Virus yields were suppressed to approximately 25% when 10 mM ammonium chloride or 10 mM methylamine was added at 1 h post infection. The presence of these bases during the first hour of infection reduced BCV yields by 34 to 37%. Amantadine was a stronger inhibitor of virus yield but this inhibitory effect was also seen in control preparations. Thus, only chloroquine suppressed BCV replication during the first hour of infection. Infected cells that were exposed to 120 µM chloroquine from the time of synchronous infection until

Table 1. Effect of lysosomotropic agents on BCV infection

Inhibitor (mM conc)	Virus yield ^a		
	full exposure	delayed exposure	% reduction ^b
Ammonium chloride (10)	15 (7.02)	23 (7.20)	34
Methylamine (10)	15 (6.53)	24 (6.73)	37
Amantadine (0.5)	5.5 (6.09)	7.0 (5.90)	22
Chloroquine (0.12)	0.1 (3.87)	6.5 (5.72)	99

^a Virus yield listed as percent of positive control and as log PFU per ml (in parentheses)

^b Percent reduction calculated as $(1.0 - [\text{full exposure}/\text{delayed exposure}])$

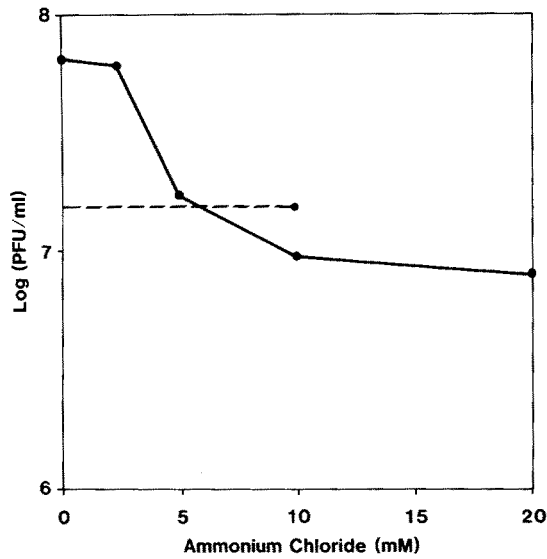


Fig. 5

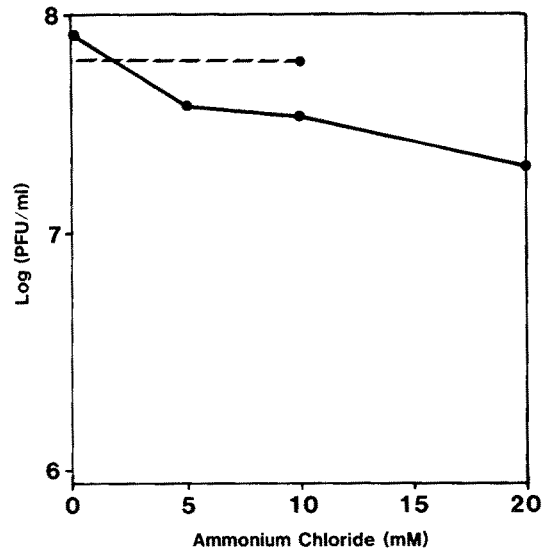


Fig. 6

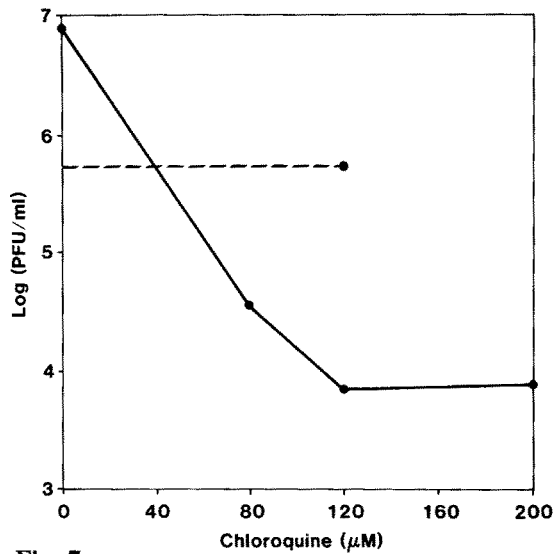


Fig. 7

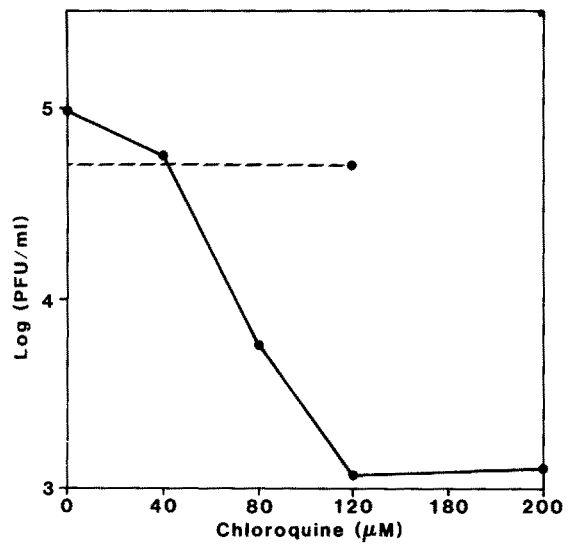


Fig. 8

Fig. 5. Effect of ammonium chloride on virus yield by infected HRT-18 cells synchronously infected with BCV. Dashed line represents virus level when 10 mM ammonium chloride was added at 1 h post infection

Fig. 6. Effect of ammonium chloride on virus yield by HRT-18 cells infected by BCV at 37°C. Dashed line represents virus level when 10 mM ammonium chloride was added at 1 h post infection

Fig. 7. Effect of chloroquine on virus yield by synchronously infected cells. Dashed line represents virus level when 120 µM chloroquine was added at 1 h post infection

Fig. 8. Effect of chloroquine on virus yield by HRT-18 cells infected at 37°C. Dashed line represents virus level when 120 µM chloroquine was added at 1 h post infection

harvest produced only 1.4% as much virus as did cultures treated with chloroquine 1 h post infection.

Synchronously BCV infected monolayers were exposed to various doses of ammonium chloride and chloroquine at the time of temperature shift to avoid drug effects on the virus adsorption stage. A second set of monolayers was pretreated with the drugs for 15 min and infected at 37 °C to ensure that intravacuolar pH levels were altered. The effects of the agents were similar for both infection protocols. Ammonium chloride reduced the yield of BCV in synchronously infected cells by less than 1 log-unit even at 20 mM levels (Fig. 5). A similar unresponsiveness to ammonium chloride treatment occurred during infection at 37 °C. Pretreatment with 10 mM ammonium chloride decreased BCV by 37% from levels produced when the agent was added after a 1 h delay (Fig. 6). Synchronous infection was strongly inhibited by 80 to 200 µM chloroquine (Fig. 7). Cells pretreated with this base and infected at 37 °C also produced less virus with increasing concentrations of the inhibitor (Fig. 8). Exposure to chloroquine at the 120 µM level resulted in the optimal reduction in virus yield. Concentrations of the drug higher than 200 µM diminished total virus yield in 1 h delay treatments to levels obtained by pretreatment. The inhibitory effect of 120 µM chloroquine on the early stages of BCV replication was therefore examined more closely in subsequent experiments.

Chloroquine inhibition of viral antigen production in infected cells

Immunofluorescence studies revealed that chloroquine treatments affected the number of BCV-infected cells in HRT-18 monolayers (Table 2). Treatments of synchronously infected cultures decreased the number of fluorescent, antigen producing cells at 12 to 36 h post infection. Replication of BCV occurred in 10 to 17% of the cell population in untreated cultures. Only 1% or less of the cell population produced BCV antigens when exposed to chloroquine at the time of infection. The numbers of fluorescent cells in the monolayers reached nearly normal levels when this treatment was delayed for 1 h even though cells vacuolization was pronounced.

Table 2. Chloroquine inhibition of antigen production

Drug exposure	% Fluorescing cells ^a		
	12 h	18 h	36 h
None	10	17	10
Full	1	0	1
Delayed	9	5	11

^a Fluorescent cell population expressed as percent of total at indicated times post infection

Time dependence of sensitivity to chloroquine inhibition

Chloroquine treatment was initiated at various times after synchronous infection (Fig. 9). Virus yields remained at low levels in cultures that were initially exposed to the drug at 5 min or less. When exposure to chloroquine was delayed until 10 min post infection, virus yield was suppressed by more than 75%. Inhibition at 50% of maximum occurred with a treatment delay of approximately 15 min. These results show that 5 to 10 min are required for infection to proceed beyond the chloroquine sensitive step in the very early stages of BCV replication. Electron microscopy revealed BCV particles progressing from the endosome to the lysosomes during this period.

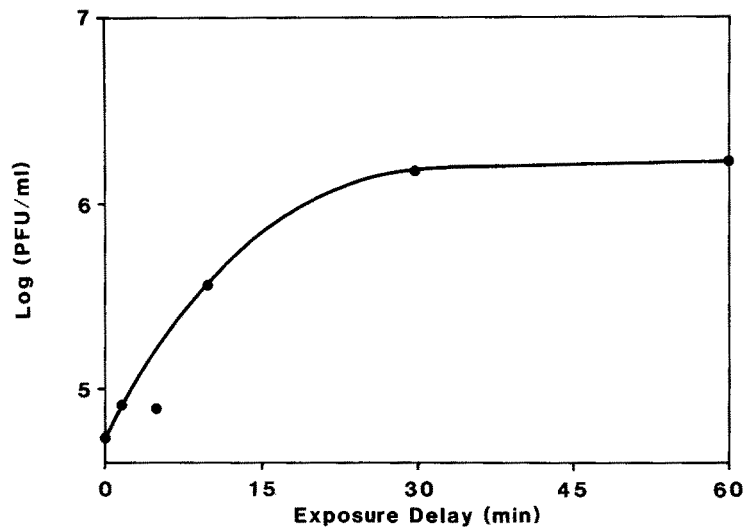


Fig. 9. Time dependence of chloroquine inhibition of BCV infection

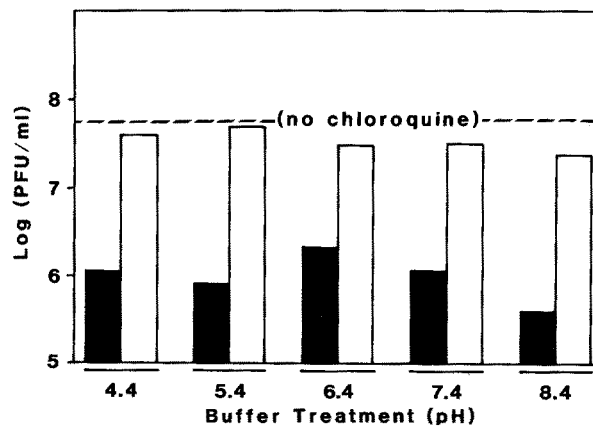


Fig. 10. Independence of chloroquine inhibition to pH treatments. Cultures were exposed to chloroquine before the buffer treatment (□) or after a delay of 1 h (■)

Independence of chloroquine inhibition to pH treatments

In an attempt to overcome the chloroquine imposed block in BCV entry, we provided conditions conducive to fusion between the plasma membrane and envelopes of infecting virions. Monolayers with virus adsorbed at 4°C were exposed to chloroquine and briefly treated with warm buffers at various pH levels to simulate conditions in intracellular vacuoles. We found that chloroquine was an effective inhibitor of BCV infection despite buffer treatments in the pH range of 4.4 to 8.4 (Fig. 10).

Discussion

Recent investigations have re-examined the role of endocytosis in infections by several animal viruses. Morphologic analyses have generally indicated that coronaviral entry is accomplished by endocytosis [3–5, 13, 26]; yet other investigations suggested that coronaviruses enter the cell by direct fusion with the plasma membrane [6, 27]. One of the objectives of our study was to employ immunolocalization to investigate the entry pathway for BCV.

Electron microscopic analysis revealed fusion of the viral envelope with the plasma membrane and confirmed that BCV particles were endocytosed by HRT-18 cells. Shortly after warming, virus particles were seen in coated pits and in small endocytic vesicles with smooth membranes. Viral particles accumulated later in structures with features of secondary lysosomes. These endocytic events resemble superficially an alternative mode for infectious entry of BCV. Gold-labeling of BCV particles was mediated by highly diluted neutralizing antibodies which did not reduce infectivity to a measurable extent. Some of the labeled virions probably represent non-infectious virus antibody-gold complexes. Their endocytosis would lead to sequestration in lysosomal compartments. However, this event appears to be irrelevant to infectious entry of BCV because we were never able to find clear morphologic evidence of fusion events along the intracellular membranes. This implies that BCV effects infectious entry by direct fusion at the cell surface.

Experiments with lysosomotropic weak bases were conducted to assess the requirement for an acidic compartment during BCV infectious entry. Our results virtually failed to reveal an unequivocal involvement of an acidic compartment. Ammonium chloride and methylamine, which raise the pH of endocytic vesicles [21], were not inhibitory for events in the first hour of BCV replication. Endocytosed viral particles reached lysosomes as early as 10 min after infection but fusion with their membrane was not observed. Although amantadine treatment from the time of infection reduced virus yield, this base was also toxic when added after a 60-min delay.

Chloroquine interfered with a relatively early stage of BCV replication as determined by the yield of infectious virus and by the number of BCV-infected cells. This effect apparently did not involve inhibition of viral envelope fusion with cell membranes. Besides raising the pH of lysosomes, chloroquine exerts

other effects on cellular functions, including inhibition of viral RNA synthesis [2]. These effects may be responsible for the 6.5% drop in BCV production when the drug is added 1 h after rewarming. We probed the chloroquine sensitivity during the very early stages of BCV infection. The kinetics of time dependence for chloroquine inhibition lead us to conclude that a sensitive step in BCV replication occurs after 5 min of infection (Fig. 9). Addition of chloroquine as late as 10 min after rewarming inhibits replication substantially [75].

In contrast, infection with Semliki Forest virus (SFV), which enters the cell by the endocytic pathway, reaches the chloroquine insensitive phase within 4 min, and later treatments with the base are relatively ineffective [8, 39, 40]. Brief treatment of SFV-adsorbed cell cultures with low pH media lifted the chloroquine block apparently by inducing virus fusion at the plasma membrane [8, 39]. The chloroquine-blocked step in BCV infection was essentially unaffected by pH treatments in the range of 4.4 to 8.4. This failure to relieve the chloroquine block in BCV replication would be expected if plasma membrane fusion with BCV is not triggered by low pH treatments. This finding is in harmony with BCV-induced cell fusion in infected bovine fetal spleen cells which fused optimally at a slightly basic pH [27], similar to a murine coronavirus-host cell system [33]. An alternative explanation for a continued chloroquine block despite low pH treatment is inhibition of events in replication subsequent to fusion. Investigators of Sindbis virus infection concluded that chloroquine inhibits only postfusion events in the replication of this virus [2]. The inhibitory activity was attributed to an effect on viral RNA synthesis rather than a block in Sindbis virus entry into the cell.

Our data indicate that BCV infection does not involve the endocytic route. Endocytosis of this virus appears to represent an abortive infection with subsequent virus degradation in lysosomes. The virions that were endocytosed were not observed to fuse with the vesicle membrane. Instead, the particles accumulated in a somewhat degraded form in lysosome-like structures. Furthermore, a low pH compartment is apparently unnecessary for BCV infection and virus-induced membrane fusion seems to be an event independent of low pH treatments. These features suggest that BCV infects cells by direct fusion with the plasma membrane. Doughri et al. [6] observed interactions of BCV strain LY-138 with the plasmalemma of infected intestinal epithelial cells and asserted that virus uptake had occurred by direct fusion with the plasma membrane. Our studies provide evidence to support that conclusion.

Note added in proof. Recently published reports [33a, 38a] describe characteristics of the mouse coronavirus spike glycoprotein E2 that are consistent with its role in infection-penetration at the plasma membrane rather than within endocytic vesicles.

Acknowledgements

This work was supported by grants 80-CRSR-2-0650, 86-CRSR-2-2871, and 89-34116-4675 from the United States Department of Agriculture. This paper contains parts of a dissertation submitted by H. R. Payne to Louisiana State University in partial fulfillment of the requirements for the Ph. D. degree.

References

1. Andersen KB, Nexø BA (1983) Entry of murine retrovirus into mouse fibroblasts. *Virology* 125: 85–98
2. Cassell S, Edwards J, Brown DT (1984) Effects of lysosomotropic weak bases on infection of BHK-12 cells by Sindbis virus. *J Virol* 52: 857–864
3. Chasey D, Alexander DJ (1976) Morphogenesis of avian infectious bronchitis virus in primary chick kidney cells. *Arch Virol* 52: 101–111
4. David-Ferreira JF, Manaker RA (1965) An electron microscope study of the development of a mouse hepatitis virus in tissue culture cells. *J Cell Biol* 24: 57–78
5. Dimmock NJ (1982) Initial stages in infection with animal virus. *J Gen Virol* 59: 1–22
6. Doughri AM, Storz J, Hajer I, Fernando HS (1976) Morphology and morphogenesis of a coronavirus infecting intestinal epithelial cells of newborn calves. *Exp Mol Pathol* 25: 355–370
7. Gonzales-Scarano F, Pobjecky N, Nathanson N (1984) La Crosse bunyavirus can mediate pH-dependent fusion from without. *Virology* 132: 222–225
8. Helenius A, Kartenbeck J, Simons K, Fries E (1980) On the entry of Semliki Forest virus into BHK-21 cells. *J Cell Biol* 84: 404–420
9. Helenius A, Marsh M, White J (1982) Inhibition of Semliki Forest virus penetration by lysosomotropic weak bases. *J Gen Virol* 58: 47–61
10. Holmes KV (1985) Replication of coronaviruses. In: Fields BN, Knipe DM, Chanock RN, Melnick J, Roizman B, Shope R (eds) *Virology*. Raven Press, New York, pp 1331–1343
11. House JA (1978) Economic impact of rotavirus and other neonatal disease agents of animals. *J Am Vet Med Assoc* 173: 573–576
12. Kielian MC, Keranen S, Kaariainen L, Helenius A (1984) Membrane fusion mutants of Semliki Forest virus. *J Cell Biol* 98: 139–145
13. Krzystniak K, Dupuy JM (1981) Early interaction between mouse hepatitis virus 3 and cells. *J Gen Virol* 57: 53–61
14. Krzystniak K, Dupuy JM (1984) Entry of mouse hepatitis virus 3 into cells. *J Gen Virol* 65: 227–231
15. Lenard J, Miller KD (1982) Uncoating of enveloped viruses. *Cell* 28: 5–6
16. Mallucci L (1966) Effect of chloroquine on lysosomes and on growth of mouse hepatitis virus (MHV-3). *Virology* 28: 355–362
17. Marsh M, Helenius A (1980) Adsorptive endocytosis of Semliki Forest virus. *J Mol Biol* 142: 439–454
18. Marsh M, Bolzau E, Helenius A (1983) Penetration of Semliki Forest virus from acidic prelysosomal vacuoles. *Cell* 32: 931–940
19. Marsh M, Matlin K, Simons K, Reggio H, White J, Kartenbeck J, Helenius A (1982) Are lysosomes a site of enveloped-virus penetration? *Cold Spring Harbor Symp Quant Biol* 46: 835–843
20. Matlin KS, Reggio J, Helenius A, Simons K (1981) Entry pathway of influenza virus in a canine kidney cell line. *J Cell Biol* 91: 601–613
21. Maxfield FR (1982) Weak bases and ionophores rapidly and reversibly raise the pH of endocytic vesicles in cultured mouse fibroblasts. *J Cell Biol* 95: 676–681
22. Mizzen L, Hilton A, Cheley S, Anderson R (1985) Attenuation of murine coronavirus infection by ammonium chloride. *Virology* 142: 378–388
23. Mollenhauer HH (1964) Plastic embedding mixtures for use in electron microscopy. *Stain Technol* 39: 111–114
24. Nemerow GR, Cooper NR (1984) Early events in the infection of human B lymphocytes by Epstein-Barr virus: the internalization process. *Virology* 132: 186–198

25. Okhuma S, Poole B (1978) Fluorescence probe measurement of the intralysosomal pH in living cells and the perturbation of pH by various agents. *Proc Natl Acad Sci USA* 75: 3327–3331
26. Patterson S, Bingham RW (1976) Electron microscope observations on the entry of avian infectious bronchitis virus into susceptible cells. *Arch Virol* 53: 267–273
27. Payne HR, Storz J (1988) Analysis of cell fusion induced by bovine coronavirus infection. *Arch Virol* 103: 27–33
28. Poste G, Pasternak CA (1978) Virus-induced cell fusion. In: Poste G, Nicholson GL (eds) *Cell surface reviews*, vol 4. Elsevier/North-Holland, Amsterdam, pp 305–357
29. Sharpee RL, Mebus CA, Bass EP (1976) Characterization of a calf diarrheal coronavirus. *Am J Vet Res* 37: 1031–1041
30. Siddell SG, Wege H, ter Meulen V (1982) The structure and replication of coronaviruses. *Curr Top Microbiol Immunol* 99: 131–163
31. Siddell SG, Anderson R, Cavanagh D, Fujiwara K, Klenk HD, Macnaughton MR, Pensaert M, Stohlman SA, Sturman L, van der Zeijst BAM (1983) Coronaviridae. *Intervirology* 20: 181–189
32. Sturman LS, Holmes KV (1982) The molecular biology of coronaviruses. *Adv Virus Res* 28: 35–112
33. Sturman LS, Ricard CS, Holmes KV (1985) Proteolytic cleavage of the E2 glycoprotein of murine coronavirus: activation of cell-fusion activity of virions by trypsin and separation of two different 90 k cleavage fragments. *J Virol* 56: 904–911
- 33a. Sturman LS, Ricard CS, Holmes KV (1990) Conformational change of the coronavirus peplomer glycoprotein at pH 8.0 and 37 °C correlates with virus aggregation and virus-induced cell fusion. *J Virol* 64: 3042–3050
34. St Cyr-Coats K, Storz J, Hussain KA, Schnorr KL (1988) Structural proteins of bovine coronavirus strain L9: effects of the host cells and trypsin treatment. *Arch Virol* 103: 35–43
35. Tompkins WAF, Watrach AM, Schmale JD, Schultz RM, Harris JA (1974) Cultural and antigenic properties of newly established cell strains from adenocarcinomas of human colon and rectum. *J Natl Cancer Inst* 52: 101–106
36. Tooze J, Tooze SA (1985) Infection of AtT20 murine pituitary tumour cells by mouse hepatitis virus strain A59: virus budding is restricted to the Golgi region. *EMBO J* 37: 203–212
37. Tycko B, Maxfield FR (1982) Rapid acidification of endocytic vesicles containing alpha-2-macroglobulin. *Cell* 28: 643–651
38. Vlasak R, Lnytzes W, Leider, J, Spaan W, Palese P (1988) The E3 protein of bovine coronavirus is a receptor-destroying enzyme with acetylsterase activity. *J Virol* 62: 4686–4690
- 38a. Weismiller DG, Sturman LS, Buchmeier MJ, Fleming JO, Holmes KV (1990) Monoclonal antibodies to the peplomer glycoprotein of coronavirus mouse hepatitis virus identify two subunits and detect a conformational change in the subunit released under mild alkaline conditions. *J Virol* 64: 3051–3055
39. White J, Kartenbeck J, Helenius A (1980) Fusion of Semliki forest virus with the plasma membrane can be induced by low pH. *J Cell Biol* 87: 264–272
40. White J, Matlin K, Helenius A (1981) Cell fusion by Semliki Forest, influenza, and vesicular stomatitis viruses. *J Cell Biol* 89: 674–679

Autors' address: H. R. Payne, Department of Neurosciences, Case Western Reserve University, Cleveland, OH 44106, U.S.A.

Received February 14, 1990